

# Fluid squeeze-out between rough surfaces: comparison of theory with experiment

B. Lorenz<sup>1,2,3</sup> and B.N.J. Persson<sup>1,3</sup>

<sup>1</sup>*IFF, FZ Jülich, D-52425 Jülich, Germany*

<sup>2</sup>*IFAS, RWTH Aachen University, D-52074 Aachen, Germany and*

<sup>3</sup>*www.MultiscaleConsulting.com*

We study the time dependency of the (average) interfacial separation between an elastic solid with a flat surface and a rigid solid with a randomly rough surface, squeezed together in a fluid. We use an analytical theory describing the fluid flow factors, based on the Persson contact mechanics theory and the Bruggeman effective medium theory, to calculate the removal of the fluid from the contacting interface of the two solids. In order to test this approach, we have performed simple squeeze-out experiments. The experimental results are compared to the theory predictions.

## 1. Introduction

Contact mechanics between solid surfaces is the basis for understanding many tribology processes[1–7] such as friction, adhesion, wear and sealing. The two most important properties in contact mechanics are the area of real contact and the interfacial separation between the solid surfaces. For non-adhesive contact and small squeezing pressure, the average interfacial separation depends logarithmically[8–10], and the (projected) contact area linearly on the squeezing pressure[11]. Here we study how the (average) interfacial separation depends on time when two elastic solids with rough surfaces are squeezed together in a fluid.

The influence of surface roughness on fluid flow at the interface between solids in stationary or sliding contact is a topic of great importance both in nature and technology. Technological applications include leakage of seals, mixed lubrication, and removal of water from the tire-road footprint. In nature fluid removal (squeeze-out) is important for adhesion and grip between the tree frog or gecko adhesive toe pads and the countersurface during rain, and for cell adhesion.

Almost all surfaces in nature and most surfaces of interest in tribology have roughness on many different length scales, sometimes extending from atomic distances ( $\sim 1$  nm) to the macroscopic size of the system which could be of order  $\sim 1$  cm. Often the roughness is fractal-like so that when a small region is magnified (in general with different magnification in the parallel and orthogonal directions) it “looks the same” as the unmagnified surface.

Most objects produced in engineering have some particular macroscopic shape characterized by a radius of curvature (which may vary over the surface of the solid) e.g., the radius  $R$  of a cylinder in an engine. In this case the surface may appear perfectly smooth to the naked eye but at short enough length scale, in general much smaller than  $R$ , the surface will exhibit strong irregularities (surface roughness). The surface roughness power spectrum  $C(\mathbf{q})$  of such a surface exhibits a roll-off wavelength  $\lambda_0 \ll R$  (related to the roll-off wavevector  $q_0 = 2\pi/\lambda_0$ ) and therefore it appears smooth (except

for the macroscopic curvature  $R$ ) on length scales much longer than  $\lambda_0$ . In this case, when studying the fluid flow between two macroscopic solids, one may replace the microscopic equations of fluid dynamics with effective equations describing the average fluid flow on length scales much larger than  $\lambda_0$ , and which can be used to study, e.g., the lubrication of the cylinder in an engine. This approach of eliminating or integrating out short length scale degrees of freedom to obtain effective equations of motion, which describe the long distance (or slow) behavior is a very general and powerful concept often used in physics.

In the context of fluid flow at the interface between closely spaced solids with surface roughness, Patir and Cheng[12, 13] have showed how the Navier-Stokes equations of fluid dynamics can be reduced to effective equations of motion involving locally averaged fluid pressures and flow velocities. In the effective equation occurs so called flow factors, which are functions of the locally averaged interfacial surface separation. They showed how the flow factors can be determined by solving numerically the fluid flow in small rectangular units with linear size of order (or larger than) the roll-off wavelength  $\lambda_0$  introduced above. In Ref. [14] one of us has developed an analytical theory for the pressure flow factors based on the Persson contact mechanics model and the Bruggeman effective medium theory to take into account the topography disorder resulting from the random roughness. We will use this theory in the calculations presented below.

This paper is organized as follows: In Sec. 2 we briefly review the basic equations of fluid dynamics and describe some simplifications which are valid for the present case. In Sec. 3 we describe the experimental method we have used to study the interfacial separation and in Sec. 4 we compare the experimental results to the theory prediction. The summary and conclusions are presented in Sec. 5.

## 2. Theory

### 2.1 Fluid flow between solids with random surface roughness

Consider two elastic solids with randomly rough sur-

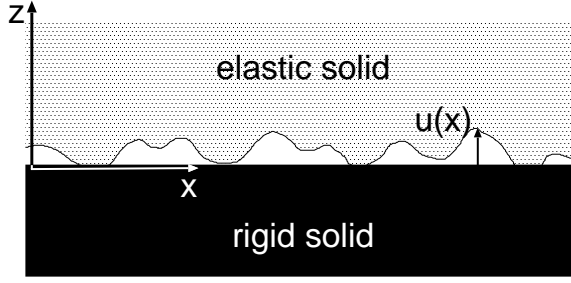


FIG. 1: An elastic solid with a rough surface in contact with a rigid solid with a flat surface.

faces. Even if the solids are squeezed in contact, because of the surface roughness there will in general be non-contact regions at the interface and, if the squeezing force is not too large, there will exist non-contact channels from one side to the other side of the nominal contact region. We consider now fluid flow at the interface between the solids. We assume that the fluid is Newtonian and that the fluid velocity field  $\mathbf{v}(\mathbf{x}, t)$  satisfies the Navier-Stokes equation:

$$\frac{\partial \mathbf{v}}{\partial t} + \mathbf{v} \cdot \nabla \mathbf{v} = -\frac{1}{\rho} \nabla p + \nu \nabla^2 \mathbf{v}$$

where  $\nu = \eta/\rho$  is the kinetic viscosity and  $\rho$  the mass density. For simplicity we will also assume an incompressible fluid so that

$$\nabla \cdot \mathbf{v} = 0$$

We assume that the non-linear term  $\mathbf{v} \cdot \nabla \mathbf{v}$  can be neglected (which corresponds to small inertia and small Reynolds number), which is usually the case in fluid flow between narrowly spaced solid walls. For simplicity we assume the lower solid to be rigid with a flat surface, while the upper solid is elastic with a rough surface. Introduce a coordinate system  $xyz$  with the  $xy$ -plane in the surface of the lower solid and the  $z$ -axis pointing towards the upper solid, see Fig. 1. The upper solid moves with the velocity  $\mathbf{v}_0$  parallel to the lower solid. Let  $u(x, y, t)$  be the separation between the solid walls and assume that the slope  $|\nabla u| \ll 1$ . We also assume that  $u/L \ll 1$ , where  $L$  is the linear size of the nominal contact region. In this case one expect that the fluid velocity varies slowly with the coordinates  $x$  and  $y$  as compared to the variation in the orthogonal direction  $z$ . Assuming a slow time dependence, the Navier Stokes equations reduces to

$$\eta \frac{\partial^2 \mathbf{v}}{\partial z^2} \approx \nabla p$$

Here and in what follows  $\mathbf{v} = (v_x, v_y)$ ,  $\mathbf{x} = (x, y)$  and  $\nabla = (\partial_x, \partial_y)$  are two-dimensional vectors. Note that  $v_z \approx 0$  and that  $p(\mathbf{x})$  is independent of  $z$  to a good approximation. The solution to the equations above can be

written as

$$\mathbf{v} \approx \frac{1}{2\eta} z(z - u(\mathbf{x})) \nabla p + \frac{z}{u(\mathbf{x})} \mathbf{v}_0 \quad (1)$$

so that  $\mathbf{v} = 0$  on the solid wall  $z = 0$  and  $\mathbf{v} = \mathbf{v}_0$  for  $z = u(\mathbf{x})$ . Integrating over  $z$  (from  $z = 0$  to  $z = u(\mathbf{x})$ ) gives the fluid flow vector

$$\mathbf{J} = -\frac{u^3(\mathbf{x})}{12\eta} \nabla p + \frac{1}{2} u(\mathbf{x}) \mathbf{v}_0 \quad (2)$$

Mass conservation demand that

$$\frac{\partial u(\mathbf{x}, t)}{\partial t} + \nabla \cdot \mathbf{J} = 0 \quad (3)$$

where the interfacial separation  $u(\mathbf{x}, t)$  is the volume of fluid per unit area. In this last equation we have allowed for a slow time dependence of  $u(\mathbf{x}, t)$  as would be the case, e.g., during fluid squeeze-out from the interfacial region between two solids.

## 2.2 Viscosity of confined fluids

It is well known that the viscosity of fluids at high pressures may be many orders of magnitude larger than at low pressures. Using the theory of activated processes, and assuming that a local molecular rearrangement in a fluid results in a local volume expansion, one expect an exponential dependence on the hydrostatic pressure  $\eta = \eta_0 \exp(p/p_0)$ , where typically (for hydrocarbons or polymer fluids)  $p_0 \approx 10^8$  Pa. Here we are interested in (wetting) fluids confined between the surfaces of elastically soft solids, e.g., rubber or gelatin. In this case the pressure at the interface is usually at most of order the Young's modulus, which (for rubber) is less than  $10^7$  Pa. Thus, in most cases involving elastically soft materials, the viscosity can be considered as independent of the local pressure. In the applications below the nominal pressure is only of order  $\sim 10^4$  Pa and the pressure in the area of real contact of order  $\sim 10^6$  Pa, so that the dependence of the (bulk) viscosity on the pressure can be neglected. Nevertheless, it has been observed experimentally[15, 16], and also found in Molecular Dynamics (MD) simulations[17, 18], that the effective viscosity  $\eta$  (defined by  $\sigma = \eta v/u$ , where  $\sigma$  is the shear stress,  $u$  the separation between the surfaces and  $v$  the relative velocity) of very thin (nanometer thickness) fluid films confined between solid walls at low pressure may be strongly enhanced, and to exhibit non-Newtonian properties. In addition, for nanometer wall-wall separations, a finite normal stress is necessary for squeeze-out, i.e., the "fluid" now behaves as a soft solid and the squeeze-out occurs in a quantized way by removing one monolayer after another with increasing normal stress[19]. In the application below we only study the (average) separation between the walls with micrometer resolution, and in this case the strong increase in the viscosity for very short wall separations becomes irrelevant.

### 2.3 Roughness on many length scales: effective equations of fluid flow

Equations (2) and (3) describe the fluid flow at the interface between contacting solids with rough surfaces. The surface roughness can be eliminated or integrated out using the Renormalization Group (RG) procedure. In this procedure one eliminate or integrate out the surface roughness components in steps and obtain a set of RG flow equations describing how the effective fluid equation evolves as more and more of the surface roughness components are eliminated. One can show that after eliminating all the surface roughness components, the fluid current [given by (2)] takes the form

$$\mathbf{J} = A(u)\nabla p + B(u)\mathbf{v} \quad (4)$$

where  $A$  and  $B$  are  $2 \times 2$  matrices, and where  $u(\mathbf{x}, t)$  and  $p(\mathbf{x}, t)$  now are *locally averaged* quantities. In general,  $A$  and  $B$  depend also on  $\nabla p$  (see Ref. [20]), but for the low pressures (and pressure gradients) prevailing in the application presented below, we can neglect this effect. If the sliding velocity  $\mathbf{v} = 0$  and if the surface roughness has isotropic statistical properties, then  $A$  is proportional to the unit matrix and is usually written as  $A = -u^3\phi_p(u)/(12\eta)$ . In this case from (3) and (4) we get

$$\frac{\partial u}{\partial t} - \nabla \cdot \left( \frac{u^3\phi_p(u)}{12\eta} \nabla p \right) = 0 \quad (5)$$

If  $u(\mathbf{x}, t)$  is independent of  $\mathbf{x}$  then (5) takes the form

$$\frac{du}{dt} - \frac{u^3\phi_p(u)}{12\eta} \nabla^2 p = 0 \quad (6)$$

In Fig. 2 we show  $\phi_p(u)$  calculated using the Persson contact mechanics and the Bruggeman effective medium theory[14]. The figure shows the dependence of  $\phi_p(u)$  on the separation  $u$  for the two (copper) surfaces used in the study below. The green curve shows the large  $u$ -behavior predicted by Tripp[21]:

$$\phi_p \approx 1 - \frac{3}{2} \frac{\langle h^2 \rangle}{u^2}$$

where  $\langle h^2 \rangle = h_{\text{rms}}^2$ . See also Ref. [14] for the calculation of higher order corrections. The small contact pressure involved in the experiments reported on below results in relative large (average) separation between the surfaces,  $u > 1.4h_{\text{rms}}$  on both surfaces (as calculated using the theory developed in Ref. [9, 10]).

### 2.4 Fluid squeeze-out

Let us squeeze a cylindrical rubber block (height  $d$  and radius  $R$ ) against a substrate in a fluid. Assume that we can neglect the macroscopic deformations of the rubber block in response to the (macroscopically) non-uniform fluid pressure. In this case  $u(\mathbf{x}, t)$  will only depend on

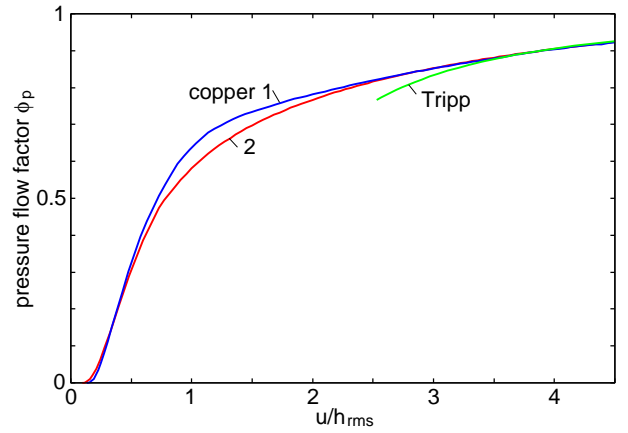


FIG. 2: The fluid pressure flow factor as a function of the average interfacial separation  $u$  divided by the root-mean-square roughness amplitude  $h_{\text{rms}}$ . For copper surfaces **1** and **2**. The green curve shows the large  $u$ -behavior predicted by Tripp[21].

time  $t$  and (6) will hold. Equation (6) imply that the fluid pressure

$$p = 2p_{\text{fluid}} \left( 1 - \frac{r^2}{R^2} \right) \quad (7)$$

where  $r = |\mathbf{x}|$  denote the distance from the cylinder axis, and where we have assumed that the external pressure vanish.  $p_{\text{fluid}}$  denotes the *average* fluid pressure in the nominal contact region. Substituting (7) in (6) gives

$$\frac{du}{dt} \approx - \frac{2u^3\phi_p(u)p_{\text{fluid}}(t)}{3\eta R^2} \quad (8)$$

If  $p_0$  is the applied pressure acting on the top surface of the cylinder block, we have

$$p_{\text{fluid}}(t) = p_0 - p_{\text{cont}}(t), \quad (9)$$

where  $p_{\text{cont}}$  is the asperity contact pressure. We first assume that the pressure  $p_0$  is so small that for all times  $u \gg h_{\text{rms}}$  and in this case  $\phi_p(u) \approx 1$ . For  $u \gg h_{\text{rms}}$  we also have[9]

$$p_{\text{cont}} \approx \beta E^* \exp \left( - \frac{u}{u_0} \right). \quad (10)$$

where  $E^* = E/(1 - \nu^2)$  (where  $E$  is the Young modulus and  $\nu$  the Poisson ratio), and where  $u_0 = h_{\text{rms}}/\alpha$ . The parameters  $\alpha$  and  $\beta$  depends on the fractal properties of the rough surface[9]. Using (10) and (9) we get from (8):

$$\frac{dp_{\text{cont}}}{dt} \approx \frac{2u^3(p_{\text{cont}}(t))}{3\eta R^2 u_0} p_{\text{cont}} (p_0 - p_{\text{cont}}), \quad (11)$$

For long times  $p_{\text{cont}} \approx p_0$  and we can approximate (11) with

$$\frac{dp_{\text{cont}}}{dt} \approx \frac{2u^3(p_0)}{3\eta R^2 u_0} p_0 (p_0 - p_{\text{cont}}).$$

Integrating this equation gives

$$p_{\text{cont}}(t) \approx p_0 - [p_0 - p_{\text{cont}}(0)] \exp\left(-\left(\frac{u(p_0)}{h_{\text{rms}}}\right)^3 \frac{t}{\tau}\right)$$

where

$$\tau = \frac{3\eta R^2 u_0}{2h_{\text{rms}}^3 p_0} = \frac{3\eta R^2}{2\alpha h_{\text{rms}}^2 p_0}. \quad (12)$$

Using (12) this gives

$$u \approx u_\infty + \left(1 - \frac{p_{\text{cont}}(0)}{p_0}\right) u_0 \exp\left(-\left(\frac{u(p_0)}{h_{\text{rms}}}\right)^3 \frac{t}{\tau}\right)$$

where  $u_\infty = u_0 \log(\beta E^*/p_0)$ . Thus,  $u(t)$  will approach the equilibrium separation  $u_\infty$  in an exponential way, and we can define the squeeze-out time as the time to reach, say,  $1.01u_\infty$ , which typically will be a few times  $\tau' = [h_{\text{rms}}/u(p_0)]^3 \tau$ . In the experiments performed below  $\eta = 100$  Pas,  $R \approx 1$  cm and  $p_0 \approx 10^4$  Pa. Using that  $u_0 \approx h_{\text{rms}}$  and that for the rough surfaces used below  $h_{\text{rms}} \approx 50$   $\mu\text{m}$ , and  $u(p_0) \approx 1.4h_{\text{rms}}$  we get  $\tau' \approx 1000$  s. Thus we expect squeeze-out to occur in about 1 hour, in good agreement with the experimental data (see below). For flat surfaces, within continuum mechanics, the film thickness approaches zero as  $t \rightarrow \infty$  as  $u \sim t^{-1/2}$ . Thus in this case there is no natural or characteristic time-scale, and it is not possible to define a meaningful fluid squeeze-out time.

At high enough squeezing pressures and after long enough time, the interfacial separation will be smaller than  $h_{\text{rms}}$ , so that the asymptotic relation (10) will no longer hold. In this case the relation  $p_{\text{cont}}(u)$  can be calculated using the equations given in Ref. [1]. Substituting (9) in (8) and measuring pressure in units of  $p_0$ , separation in units of  $h_{\text{rms}}$  and time in units of  $\tau$  one obtain

$$\frac{du}{dt} \approx -\alpha^{-1} \phi_p(u) u^3 (1 - p_{\text{cont}}), \quad (13)$$

where  $\alpha = h_{\text{rms}}/u_0$ . This equation together with the relation  $p_{\text{cont}}(u)$  constitute two equations for two unknown ( $u$  and  $p_{\text{cont}}$ ) which can be easily solved by numerical integration.

### 2.5 Rubber block under vertical loading

Consider a cylindrical rubber block (radius  $R$ , height  $d$ ) squeezed between two flat surfaces. If both surfaces are lubricated (no friction) the stress at the interfaces will be constant  $p = p_0 = F_N/\pi R^2$  and the change in the thickness  $\Delta d$  (assuming linear elasticity) will be determined by  $p_0 = E\Delta d/d$ . However, if the rubber adhere (or is glued) to the upper surface with no-slip the situation may be very different[22, 23]. If  $d > R$  the stress at the (lower) interface will again be nearly uniform and  $\Delta d$  will be determined by  $p_0 = E_{\text{eff}}\Delta d/d$  where

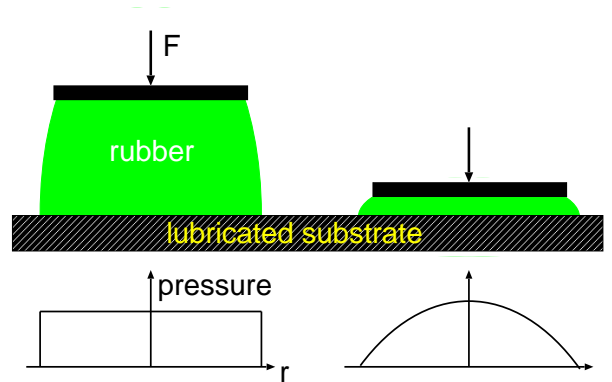


FIG. 3: A cylindrical rubber block (height  $d$  and radius  $R$ ) squeezed against a lubricated substrate (no friction). If  $d > R$  the pressure distribution at the interface will be nearly uniform (left) while if  $d \ll R$  (right) the pressure distribution will be nearly parabolic. We have assumed that the upper surfaces of the rubber cylinders are glued (no slip) to a flat rigid disk.

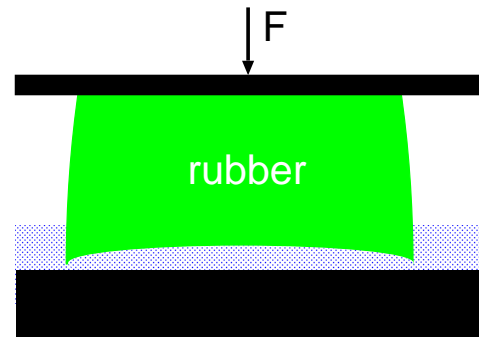


FIG. 4: The non-uniform hydrodynamic pressure is highest at the center of the contact region and will deform the rubber block as indicated in the figure.

$E_{\text{eff}} > E$  but nearly identical to  $E$ . In the opposite limit of a very thin rubber disk,  $d \ll R$ , the pressure distribution at the bottom surface will be nearly parabolic  $p(r) \approx 2p_0[1 - (r/R)^2]$  (see Fig. 3) and the effective elasticity  $E_{\text{eff}} \gg E$ . Experiments have shown that when a rubber disk is squeezed against a rough surface, even if the rubber disk is very thin, the (locally averaged) pressure distribution at the bottom surface of the rubber disk will be nearly constant[24]. This is because the rubber is pressed into the ridges on the rough surface under vertical loading, and the hydrostatic pressure becomes smaller. We also note that while  $E_{\text{eff}} > E$  determines the change in the thickness of the rubber block, the local elastic asperity-induced deformations at the (lower) interface will be determined (to a good approximation) by the Young's modulus  $E$ .

In Sec. 2.4 we have shown that a flat cylinder sur-

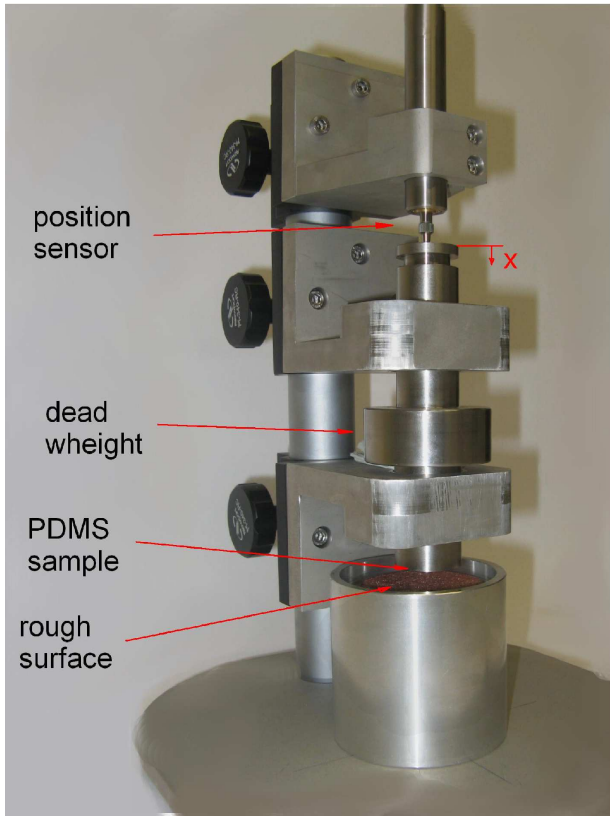


FIG. 5: Experimental set-up for studies of fluid squeeze-out between surfaces of elastic solids.

face squeezed against a flat substrate in a (Newtonian) fluid gives rise to a parabolic fluid pressure distribution. This implies that for a very thin ( $d \ll R$ ) elastic disk, glued to a flat rigid surface, and squeezed against another flat surface in a fluid, we expect the bottom surface of the elastic disk to remain nearly flat and the assumption made in Sec. 2.4 will hold to good accuracy. However, if the rubber block is thick enough ( $d > R$ ) the bottom surface of the block will bend inwards as indicated in Fig. 4, which will slow down the fluid squeeze-out.

### 3. Experimental

We have studied the squeeze-out of fluids between solids with rough surfaces as shown in Fig. 5. In the experimental set-up a cylindrical silicon rubber block is squeezed against a rough counter-surface in the presence of a fluid. The rubber block is attached to a dead weight, resulting in the driving force  $F_N = 13.8$  N. This force is kept constant for all experiments. We have measured the downwards movement of the dead weight as a function of time using a digital gauge with a relative position resolution of  $0.5 \mu\text{m}$ . In order to slow down the whole process, we use a very high viscosity silicon oil (Dow Corning 200 Fluid, viscosity 100 Pas) and a relative low nominal squeezing pressure (about  $10^4$  Pa). In the different configurations we either squeeze an elastic silicon rubber

block, or a rigid glass block, against smooth (glass) or rough (copper) surfaces in order to test different aspects of the squeeze-out. The rubber blocks have the radius  $R = 1.5$  cm and height  $d = 1$  cm,  $0.5$  cm and  $0.3$  cm. We use a silicone elastomer (PDMS) prepared using a two-component kit (Sylgard 184) purchased from Dow Corning (Midland, MI). This kit consists of a base (vinyl-terminated polydimethylsiloxane) and a curing agent (methylhydrosiloxane-dimethylsiloxane copolymer) with a suitable catalyst. From these two components we prepared a mixture 10:1 (base/cross linker) in weight. The mixture was degassed to remove the trapped air induced by stirring from the mixing process and then poured into cylindrical casts. The bottom of these casts was made from glass to obtain smooth surfaces (negligible roughness). The samples were cured in an oven at  $80^\circ\text{C}$  for over 12 hours. The rough copper surfaces were prepared by pressing sandpaper surfaces against flat and plastically soft copper surfaces using a hydraulic press. Using sandpaper with different grit size, and repeating the procedure many times, resulted in (nearly) randomly rough surfaces suitable for our experiment.

The silicon block was placed in the high viscosity fluid with some distance to the rough surface. In order to avoid kinetic (inertia) effects the initial separation was selected to be very small. The nominal force was applied by dropping the dead weight with the rubber block attached to it. The displacement of the dead weight from its starting position was measured as a function of time.

In Fig. 7 we show the power spectrum of the two rough copper surfaces **1** and **2** used in our study. The area of real contact (at the nominal squeezing pressure  $\approx 2 \times 10^4$  Pa) as a function of the magnification  $\zeta$  is shown in Fig. 8. Note that the area of real contact (i.e., the contact area at the highest magnification  $\zeta_1$  or wavevector  $q_1 = q_0 \zeta_1$ ) is rather similar in both cases (equal to  $A = 0.016A_0$  and  $0.013A_0$  for surfaces **1** and **2**, respectively) in spite of the rather large difference in the rms roughness values ( $h_{\text{rms}} = 42$  and  $88 \mu\text{m}$ , respectively). This is due to the fact that the rms roughness is dominated by the longest wavelength roughness components, while the area of real contact is strongly influenced by the short wavelength roughness components, which are very similar on both surfaces (see Fig. 7 for large wavevector). The small contact pressure result in relative large (average) separation between the surfaces,  $\bar{u} \approx 1.4h_{\text{rms}}$  on both surfaces (as calculated using the theory developed in Ref. [9, 10]).

### 4. Comparison of theory with experiment

In Fig. 9 we show the surface separation as a function of the logarithm of time when a glass and a PDMS cylindrical block are squeezed against a flat glass substrate in a silicon oil. Also shown is the theoretical prediction (lower curve). The cylinder is  $d = 0.5$  cm thick and has the diameter  $D = 2R = 3$  cm. As expected, the theory

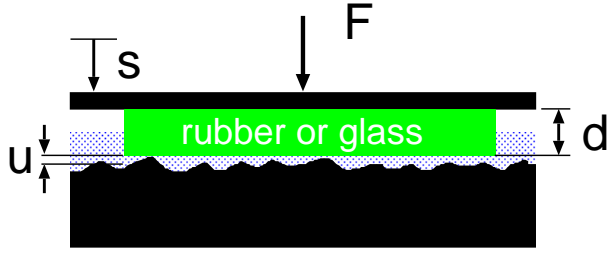


FIG. 6: Squeeze-out experimental set-up. A cylindrical glass or rubber block is squeezed against a substrate with a smooth or rough surface in a fluid. The cylindrical body has the height  $d = 0.5$  cm thick and the diameter  $D = 2R = 3$  cm. The normal load  $F_N = 13.8$  N and the fluid viscosity  $\eta = 100$  Pas. The vertical displacement  $u$  of the upper surface is registered as a function of time.

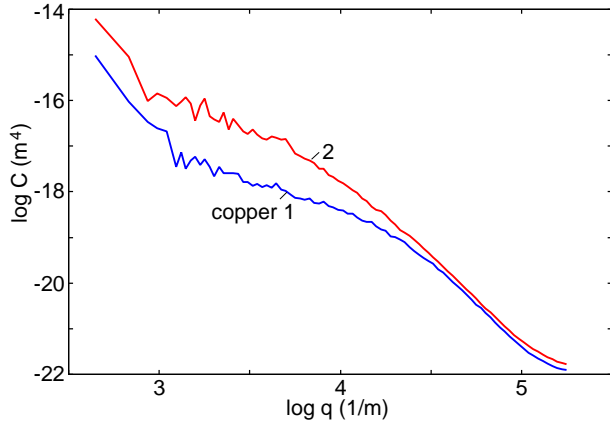


FIG. 7: The logarithm of the surface roughness power spectrum as a function of the logarithm of the wavevector for two copper surfaces, **1** and **2**, with the root-mean-square roughness  $42 \mu\text{m}$  and  $88 \mu\text{m}$ , respectively.

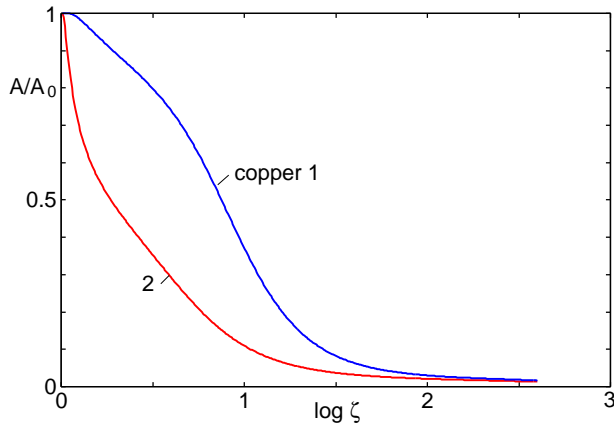


FIG. 8: The calculated relative area of contact  $A/A_0$  (where  $A_0$  is the nominal contact area) when a glass and a PDMS block is squeezed against two copper surfaces **1** and **2** with surface roughness produced as described in the text.

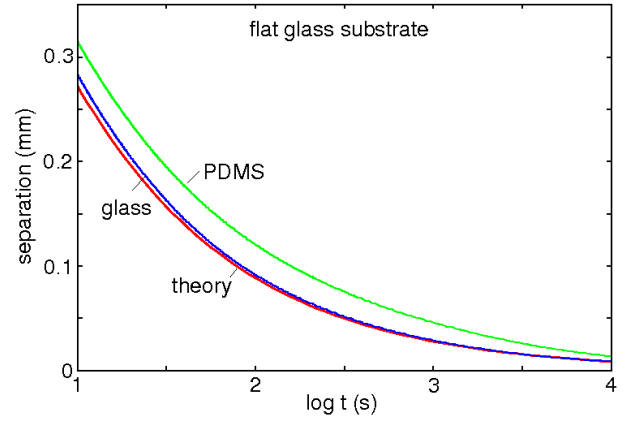


FIG. 9: The surface separation as a function of the logarithm of time when a glass and a PDMS cylindrical block is squeezed against a flat glass substrate in a silicon oil. Also shown is the theoretical prediction (lower curve). The cylindrical body has the height  $d = 0.5$  cm thick and has the diameter  $D = 2R = 3$  cm. The normal load  $F_N = 13.8$  N and the fluid viscosity  $\eta = 100$  Pas.

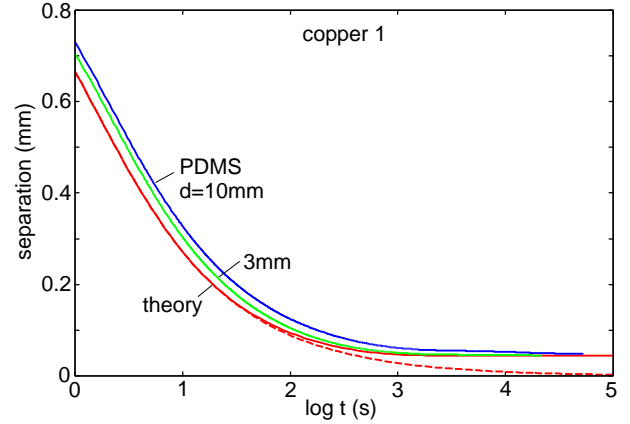


FIG. 10: The surface separation as a function of the logarithm of time when PDMS cylindrical blocks with thickness 10 mm and 3 mm are squeezed against a rough copper surface **1** (root-mean-square roughness  $h_{\text{rms}} = 42 \mu\text{m}$ ) in a silicon oil. Also shown is the theoretical prediction for a flat substrate (dashed curve) and for the copper surface **1** (lower solid curve).

result agree almost perfectly with the experimental results for the glass cylinder (no fitting parameters), but for the rubber block the (average) separation is larger and the squeeze-out slower. We attribute this to temporarily trapped fluid resulting from the upward bending (before contact with the substrate) of the bottom surface of the rubber block as in Fig. 4. We define the “trapped” fluid volume  $\Delta V$  as the fluid volume between the bottom surface of the block and a flat (mathematical) surface in contact with the block at the edge  $r = R$  of the bottom surface of the block. Using the theory of elasticity  $\Delta V = \pi R^2 \delta$  with  $\delta = CR\bar{p}/E_{\text{eff}}$ , where  $C$  is a con-

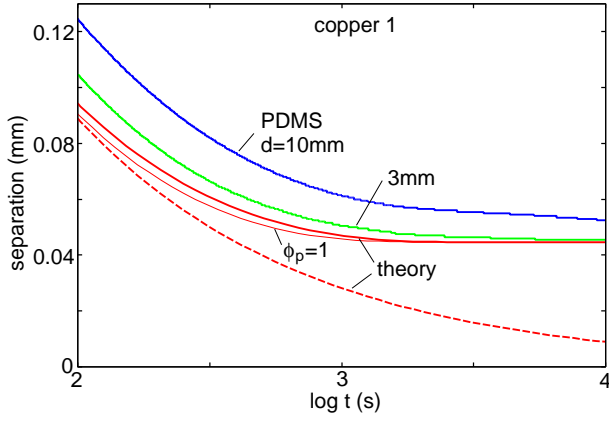


FIG. 11: The same as in Fig. 10 but for a more narrow time interval. The thin solid line is the calculated squeeze-out when the pressure flow factor  $\phi_p(u) = 1$

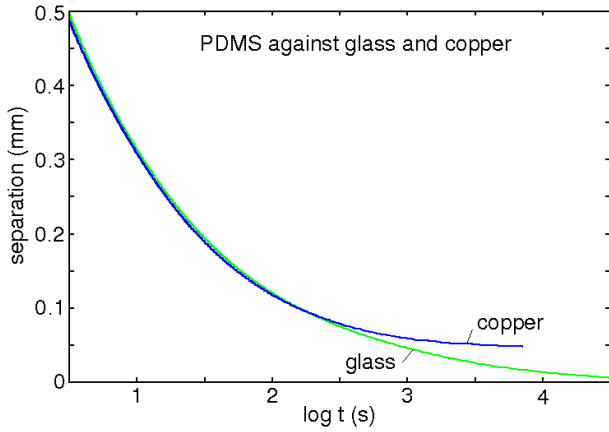


FIG. 12: The surface separation as a function of the logarithm of time when a  $d = 0.5$  cm thick PDMS cylindrical block is squeezed against a flat glass substrate (lower curve), and against the (rough) copper surface **1** (root-mean-square roughness  $h_{\text{rms}} = 42 \mu\text{m}$ ) in a silicon oil.

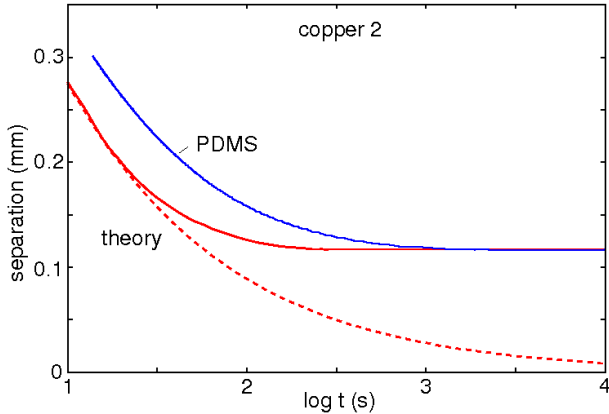


FIG. 13: The surface separation as a function of the logarithm of time when a  $d = 0.5$  cm thick PDMS cylindrical block is squeezed against the rough copper surface **2** (root-mean-square roughness  $h_{\text{rms}} = 88 \mu\text{m}$ ) in a silicon oil. Also shown is the theoretical prediction (lower curve).

stant of order unity. For the rubber block with thickness  $d = 0.5$  cm we get  $E_{\text{eff}} \approx E[1 + 0.5 \times (R/2d)^2] \approx 4$  MPa and  $\delta \approx 40 \mu\text{m}$ , resulting in an increase in the average interfacial separation by  $\sim 40 \mu\text{m}$ , which is consistent with what we observe.

Fig. 10 and 11 show the surface separation as a function of the logarithm of time when PDMS cylindrical blocks with thickness 1 cm and 0.3 cm are squeezed against the rough copper surface **1** (root-mean-square roughness  $h_{\text{rms}} = 42 \mu\text{m}$ ) in a silicon oil. Also shown is the theoretical prediction for a flat substrate (dashed curve) and for the copper surface (lower solid curve), assuming that the bottom surface of the rubber disk is macroscopically flat. Note that the agreement between the theory and experiment is much better for the thinner rubber disk. This is indeed expected since the fluid-pressure induced curvature of the bottom surface of the rubber is smaller for the thin rubber disk (see Sec. 2.5). But even for the thin rubber disk some fluid-pressure induced bending of the bottom surface of the rubber disk is expected, and we believe this is the main origin for the slightly slower squeeze-out observed in the experiment as compared to the theory prediction. The thin solid line Fig. 11 shows the calculated squeeze-out when the pressure flow factor  $\phi_p(u) = 1$ . In the present case the pressure flow factor is close to unity and this explains the relative small difference between using  $\phi_p = 1$  (thin red line) and using the calculated  $\phi_p(u)$  (from Fig. 2) (thick red line).

In Fig. 12 we show the surface separation as a function of the logarithm of time when the  $d = 0.5$  cm thick PDMS disk is squeezed against a flat glass substrate (lower curve), and against the (rough) copper surface **1** (root-mean-square roughness  $h_{\text{rms}} = 42 \mu\text{m}$ ) in a silicon oil. Note that before contact with the substrate, the fluid-pressure induced bending of the bottom surface of the block is the same in both cases (giving overlapping curves for  $t < 300$  s).

In Fig. 13 we show the surface separation as a function of the logarithm of time when the  $d = 0.5$  cm thick PDMS cylindrical block is squeezed against the (rough) copper surface **2** (root-mean-square roughness  $h_{\text{rms}} = 88 \mu\text{m}$ ) in a silicon oil. Also shown is the theoretical prediction (lower curve). Again, the bending of the bottom surface of the rubber block results in a slower squeeze-out than predicted theoretically assuming a (macroscopically) flat bottom surface of the rubber block.

## 5. Summary and conclusion

In this paper we have studied the fluid squeeze-out from the interface between an elastic block with a flat surface and a randomly rough surface of a rigid solid. We have calculated the (average) interfacial separation as a function of time by considering the fluid flow using a contact mechanics theory in combination with thin-film hydrodynamics with flow factors (which are functions of

the (local) interfacial separation) obtained using a recently developed theory. We have explained the importance of the large length-scale elastic deformations on the squeeze out.

The theoretical results have been compared to experimental results. The experiment was performed by squeezing cylindrical rubber blocks with different height  $d$  against rough cooper surfaces in the presents of a high viscosity fluid (silicone oil). Changing the height  $d$  of the rubber block, and also performing additional experiments with flat against flat surfaces, with combinations of rigid-rigid and elastic-rigid, we could show the importance of both the large length-scale and asperity induced elastic deformation on the squeeze-out. In particular, large length-scale deformations of the bottom surface of the rubber block resulted in (temporary) trapped fluid between the elastic solid and the rigid countersurface, which drastically slowed-down the squeeze-out. This effect is smallest for the thinnest rubber block, for which case we find good agreement between the theory (where we have neglected the large length-scale deformations of the rubber block) and the experiments. Another mechanism which drastically slows down the squeeze-out occurs at much higher nominal pressure (or load) than used in the present experiment. This is due to sealed-off fluid in the nominal contact region during contact formation. This effect occurs when the area of real contact approaches  $\approx 0.4A_0$ , where the area of real contact percolate resulting in sealed-off regions of fluid, which may disappear only extremely slowly, e.g., by diffusion into the rubber. This effect was discussed in Ref. [25] and seems to be of importance in many applications involving high contact pressures, e.g., it may result in a static (or start-up) friction force which slowly increases with time even after very long time (say one year).

The squeeze-out of fluids from the interfacial region between elastic solids with rough surfaces is very important in many technical applications (e.g. a tires rolling on a wet road, wipers and dynamic seals), and the results presented in this paper contribute to this important subject.

### Acknowledgments

This work, as part of the European Science Foundation EUROCORES Program FANAS, was supported from funds by the DFG and the EC Sixth Framework

Program, under contract N ERAS-CT-2003-980409.

- 
- [1] B.N.J. Persson and C. Yang, *J. Phys.: Condens. Matter* **20**, 315011 (2008)
  - [2] B.N.J. Persson, *J. Phys.: Condens. Matter* **20**, 315007 (2008)
  - [3] F.P. Bowden and D. Tabor, *Friction and Lubrication of Solids* (Wiley, New York, 1956).
  - [4] K.L. Johnson, *Contact Mechanics*, (Cambridge University Press, Cambridge, 1966).
  - [5] B.N.J. Persson, *Sliding Friction: Physical Principles and Applications*, 2nd edn. (Springer, Heidelberg, 2000).
  - [6] J.N. Israelachvili, *Intermolecular and Surface Forces* (Academic, London (1995)).
  - [7] See, e.g., B.N.J. Persson, O. Albohr, U. Tartaglino, A.I. Volokitin and E. Tosatti, *J. Phys. Condens. Matter* **17**, R1 (2005).
  - [8] B.N.J. Persson, *Surface Science Reports* **61**, 201 (2006).
  - [9] B.N.J. Persson, *Phys. Rev. Lett.* **99**, 125502 (2007)
  - [10] C. Yang and B.N.J. Persson, *J. Phys. Condens. Matter* **20**, 215214 (2008).
  - [11] B.N.J. Persson, *J. Chem. Phys.* **115**, 3840 (2001).
  - [12] N. Patir and H.S. Cheng, *Journal of Tribology, Transactions of the ASME* **100**, 12 (1978).
  - [13] N. Patir and H.S. Cheng, *Journal of Tribology, Transactions of the ASME* **101**, 220 (1979).
  - [14] B.N.J. Persson, *J. Phys.: Condens. Matter* **22**, 265004 (2010).
  - [15] S. Yamada, *Tribology Letters* **13**, 167 (2002).
  - [16] L. Bureau, *Phys. Rev. Lett.* **104**, 218302 (2010).
  - [17] P.A. Thompson, G.S. Grest and M.O. Robbins, *Phys. Rev. Lett.* **68**, 3448 (1992).
  - [18] I.M. Sivebaek, V.N. Samoilov and B.N.J. Persson, in preparation.
  - [19] B.N.J. Persson and F. Mugele, *J. Phys.: Condens. Matter* **16**, R295 (2004).
  - [20] M. Scaraggi, G. Carbone, B.N.J. Persson and D. Dini, *subm. to Soft Matter*.
  - [21] J.H. Tripp, *ASME J. Lubrication Technol.* **105**, 485 (1983).
  - [22] A.N. Gent, *Rubber Chem. Technol.*, **67**, 549 (1994).
  - [23] J.B. Suh, *Stress analysis of rubber blocks under vertical and shear loading*, PhD thesis (2007).  
<http://etd.ohiolink.edu/view.cgi?akron1185822927>
  - [24] E.A. Sakai, *Tire Science and Technology* **23**, 238 (1995).
  - [25] B. Lorenz and B.N.J. Persson, *European Journal of Physics* **E32**, 281 (2010).